6. Spencer R. M., Christopher O. Method and system for locating and positioning circular workpieces: Pat. No. US4833790A USA. No. 48,194; declareted: 11.05.1987; published: 30.05.1989.
7. Influence assessment of metal-cutting equipment geometrical accuracy on OMV-technologies accuracy / Koltsov A. G., Blokhin D. A., Krivonos E. V., Narezhnev A. N. // 2016 Dynamics of Systems, Mechanisms and Machines (Dynamics). 2016. doi: https://doi.org/10.1109/dynamics.2016.7819029
8. Radu P. Adaptive Machining for High Precision Fabrication. URL: http://www.mapyourshow.com/MYS_Shared/imts16/handouts/RaduPavelIMTS57.pdf
9. Petrakov Y., Shuplietsov D. Programming of adaptive machining for end milling // Mechanics and Advanced Technologies. 2017. Vol. 1, Issue 79. P. 34–40. doi: https://doi.org/10.20535/2521-1943.2017.79.97342
10. Lee S.-K., Ko S.-L. Development of simulation system for machining process using enhanced Z map model // Journal of Materials Processing Technology. 2002. Vol. 130-131. P. 608–617. doi: https://doi.org/10.1016/s0924-0136(02)00761-6
11. Calculating the Hausdorff distance between curves / Belogay E., Cabrelli C., Molter U., Shonkwiler R. // Information Processing Letters. 1997. Vol. 64, Issue 1. P. 17–22. doi: https://doi.org/10.1016/s0020-0190(97)00140-3
12. Guthe M., Borodin P., Klein R. Fast and accurate Hausdorff distance calculation between meshes // Conference proceedings. 2005.

UDC 621.914.1
DOI: 10.15587/1729-4061.2019.163325

IMPROVING EFFICIENCY OF MACHINING THE GEOMETRICALLY COMPLEX SHAPED SURFACES BY MILLING WITH A FIXED SHIFT OF THE CUTTING EDGE

A. Skorkin
PhD*
E-mail: Andromeda862@ukr.net
O. Kondratyuk
PhD*
N. Lamnauer
Doctor of Technical Sciences**
V. Burdeinaya
PhD**
*Department of Machine Building and Transport***
Department of Labor Protection, Standardization and Certification*
***Ukrainian Engineering Pedagogics Academy
Universitetska str., 16, Kharkiv, Ukraine, 61003

Для підвищення ефективності обробки фрезеруванням складних фасонних поверхонь (СФП), застосовуються в основному методи, пов'язані з поліпшенням властивостей інструментального матеріалу, зміною складу та властивостей поверхневого шару інструменту, нанесенням тонкоплівкових покриттів, зниженням шорсткості робочих поверхонь і поліпшенням умов експлуатації інструменту застосуванням ЗОТС.

Виходячи з вище викладеного в роботі досліджені та викладені науково обґрунтовані технічні та технологічні рішення, які полягають в розробці нового високоефективного способу обробки складних фасонних поверхонь дисковими радіусними фрезами зі зворотно-гойдальним рухом подачі. Даний метод обробки дозволяє підвищити період стійкості інструменту в 1,7 рази і продуктивність фрезерування в 1,6 рази, за рахунок постійного кінематичного зсуву ріжучої крайки відносно поверхні різання.

Запропоновано математичний апарат способу фрезерування з постійним зсувом ріжучої крайки. Аналіз даного методу за допомогою числових функцій, дозволив встановити аналітичні залежності для визначення товщини та об'єму одиничного зрізаємого шару.

Основний вплив на величину товщини зрізаного шару надає подача на зуб Sz, а на обсяг – кут υ, що визначає нормальні умови різання. Досліджено модель розподілу теплових потоків в ріжучому клині для способу фрезерування зі зворотно-гойдальним рухом подачі, що враховує амплітуду руху, що гойдає заготовки. Встановлено зниження температури до 330,2...395,5 °C, тобто на 80,6...181,6 °C для штампової сталі 9ХС і до 193,8...285 °C, тобто 56,6...120,2 °C для стали 45, в порівнянні зі звичайним фрезеруванням. Встановлено, що загальна довжина ріжучої крайки збільшується в 2,4 рази, при цьому температура знижується в 1,5 рази

Ключові слова: фрезерування, кінематична схема різання, ріжучий інструмент, ріжуча крайка, складна фасонна поверхня, ЧПУ

1. Introduction

Kinematic schemes of surface machining, cutting tool designs and initial tool surfaces directly affect durability of the cutting tool material and, consequently, machining efficiency. For example, when 20CR13 steel is machined by means of a carbide tool, transition from kinematic schemes with a continuous cutting process (turning with a cutter) to intermittent machining (turning with a milling cutter) reduces total path of the tool up to 50 times [1–3].

This is evidenced by the fact that tool wear is greatly influenced by the tool type, geometry and design, method of incision into the workpiece, type of equipment, etc. As is well known, milling cutters (mills) working in conditions of intermittent cutting undergo impact at the moment of their coming into contact with the workpiece. Durability of mills during face milling with straight cuts of cast iron [4] as well as carbon and low alloy steels is higher when milling with a minimum thickness of the cut (Fig. 1, *b*).

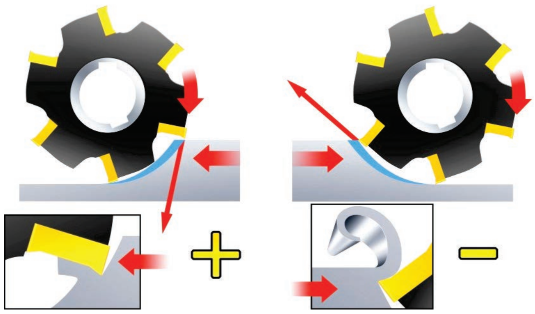

Fig. 1. Methods of milling determined by direction of motion of the workpiece relative to the tool; down milling (*a*); up milling (*b*)

Conditions of entering of the carbide insert into the cutting zone are more favorable in down milling (Fig. 1, *a*). It is possible to avoid high temperatures in the cutting zone and minimize susceptibility of the workpiece material to hardening. Bigger thickness of chips is an advantage in this case. Cutting forces press the workpiece to the machine table and the inserts to the mill body seats contributing to their reliable fixation.

Down milling is preferable provided that the strength of equipment, fastening and the material being machined make this method applicable. At the same time, this process is associated with certain difficulties. Cutting forces tend to draw the mill into the machining allowance and press the workpiece down. In the event of vibration hazard, down milling is more favorable [5–7].

At present, there is a real possibility of controlling parameters of the part surface layer in the process of its manufacture. This possibility can be realized by rational choice of methods and conditions of preliminary and final machining of the part working surfaces. In this case, various procedures are used for ensuring parameters of the part surface layer taking into consideration the part operation conditions.

There are now many various schemes of surface shaping. Most of these schemes are united by the fact that shaping is realized by three coordinated motions:

– rotational motion (machining by disk tools);
– rotary motion of the workpiece;
– translational motion of the workpiece or the tool along the axis of the shaped surface coordinated with the rotary motion.

The process of lathing shaped surfaces in which cutting blade cuts to the entire depth of the profile is the exception.

The most promising way is machining of geometrically complex shaped surfaces by means of a disk mill with a combined working surface. This method of machining geometrically complex surfaces makes it possible to improve accuracy due to rolling-off the part profiles with rectilinear generatrixes of the tools. Besides, it is a versatile and highly productive method. Disadvantage of this method consists in inappropriateness of machining concave curvilinear profiles since only a small toroidal portion of the working surface will participate in machining [8].

A large number of applied kinematic schemes of machining shaped surfaces is largely caused by distinctly differing part dimensions. Choice of the most rational machining method and its parameters is a rather intricate problem which was not given due attention till now.

2. Literature review and problem statement

To date, there are multitudes of schemes of shaping geometrically complex shaped surfaces including screw surfaces [9]. Conventional and simplest method of machining the shaped part surface and programming path of the mill motion consists in copying the profile accompanied by numerous motions of the mill into and off the contact with the workpiece (Fig. 2).

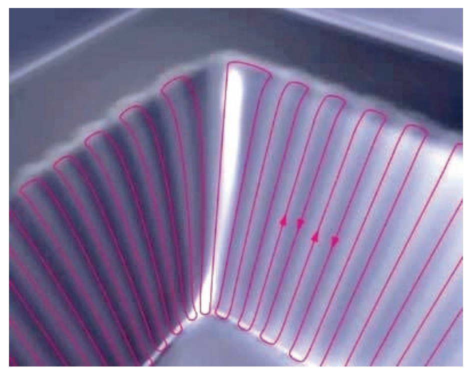

Fig. 2. Copying method

Disadvantage of this method consists in low durability of the cutting tool because of occurrence of high loads in the center of the mill and longer duration of the machining cycle.

Milling with a disk cutter or a milling head is the more versatile method for machining shaped surfaces. Most often, when milling some parts (for example, spiral drills), the angle set between the mill and the axis of the drill, ω1, is chosen 1–2° larger or smaller than the angle of lift of the helical line, ω. This approach provides the best quality of the helical surface and improves durability of the tool but only if the profile distortion and undercut are excluded [10].

Trochoidal milling can be described as the circle milling with a simultaneous linear motion. The mill removes repetitive material «layers» at the expense of successive spiral passages in a radial direction. Compared with conventional grooving, the trochoidal method provides greater stability of the process, tool durability and lower tool costs.

When milling grooves with a width less than $2D_Ф$ (Fig. 3), a single continuous spiral passage in radial direction is programmed to form profile. In this case, the feed value is constant and the radial cut depth is variable. The time when the tool is out of cutting is equal to 50 % of the total cycle time.

For grooves wider than $2D_Ф$ (Fig. 4), spiral passage similar to that used in machining narrow grooves at which 50 % of the time is spent on taking the tool from the cutting zone can be optimized by increasing the passage width [11].

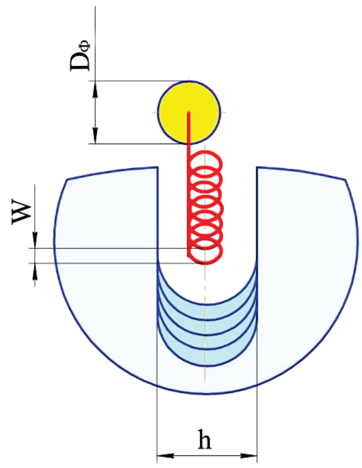

Fig. 3. Schematic of trochoidal milling of a narrow groove

Fig. 4. Schematic of trochoidal milling of a wide groove

In the process of cutting, the tool working surfaces are in extreme conditions of friction and wear. Their wear is mainly determined by the effect of elevated temperatures and contact pressures in the tool and material interaction zone [12]. Heat phenomena directly affect nature of chip and burr formation, cutting forces and microstructure of the surface layer. Heat emission during cutting is explained by the fact that mechanical energy spent on chipping converts into heat. When cutting, a complex interweaving of heat flows takes place and heat from each source is distributed among all bodies involved in the cutting process (chips, workpiece, tool) [13].

Cutting speed has the strongest effect on temperature: with an increase in speed, temperature initially increases rapidly and then asymptotically tends to a limiting value that is approximately equal to the machined material melting point.

In conditions of intermittent cutting, cutting with replaceable inserts, short-time and periodic cutting, magnitudes of heat flows and cutting temperature vary in time, that is, unstable heat exchange occurs (Fig. 5, 6). As a result, cutting temperature depends not only on the machining conditions and physical and mechanical properties of the material being machined but also on cooling conditions during the idle run [14, 15].

Tool durability can be increased by reducing temperature in the cutting zone through a change of kinematics of the cutting tool motion.

Large chip thickness leads to a decrease in the tool lifetime and can cause quick failure of the tool. It can be noticed that if the program involves entry into the workpiece in a straight path, thick chips are formed until the mill fully enters into the workpiece. As a result, the tool lifetime is quickly reduced. To ensure acceptable lifetime, it will be necessary to reduce feed rate for the entire process (Fig. 7, *b*).

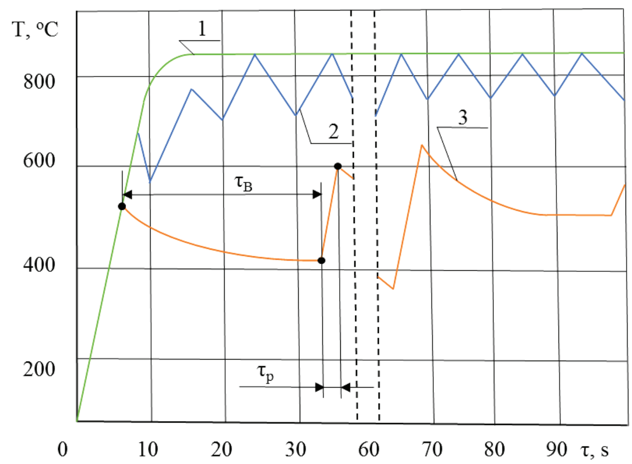

Fig. 5. Variation of temperature of the cutting edge of TI14CO8 carbide tool depending on heat exchange conditions: stable (1); unstable (2, 3)

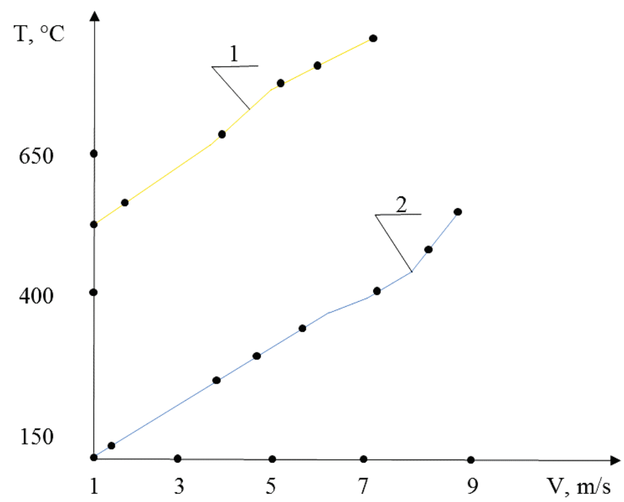

Fig. 6. Dependence of temperature of the TI14CO8cutter on the speed of cutting: prismatic cutting (1); rotational cutting (2)

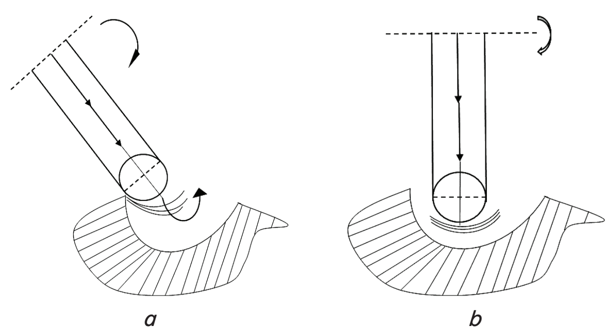

Fig. 7. The path of mill entry into the workpiece: mill entry by a curvilinear path (*a*); entire mill entry by a straight-line path (*b*)

There are two ways to solution of this common problem. They make it possible to apply an optimal feed rate during the cutter entry into the workpiece:

– programming for a straight-line entry path but with the feed rate reduced by 50 % until complete cutter entry in the workpiece occurs;

– curvilinear entry path with a clockwise rotation (counterclockwise rotation does not help solve the problem of formation of thick chips) (Fig. 7, *a*).

It can be noticed that when a curvilinear entry path takes place, thickness of the chips at their end is always zero. This fact enables use of high feed rates and extends the tool lifetime.

An analysis of existing methods of machining geometrically complex shaped surfaces by edge cutting machining indicates that wear of inserts is concentrated mainly at their apex. For a more even wear of the cutting insert, the tool is subjected to a rolling motion of the cutting edge over the machined surface. These methods are poorly studied. They include methods of linear or nonlinear rolling in which working surface of the tool rolls over the nominal surface of the part. It is assumed that shift of the cutting edge and periodic replacement of the main cutting edge sections by auxiliary sections and vice versa should significantly improve the tool durability.

3. The aim and objectives of the study

The study objective is to determine ways of improving the tool wear resistance and efficiency when milling geometrically complex shaped surfaces by means of a fixed shift of the cutting edge relative to the cutting surface.

To achieve this objective, the following tasks were solved:

– to develop a new method of milling of geometrically complex shaped surfaces with the use of a kinematic scheme that provides fixed shift of the cutting edge relative to the cutting surface;

– to develop an algorithm of calculation of the path of tool motion during milling with a fixed shift of the cutting edge relative to the cutting surface.

4. The methods used to study the machining of shaped surfaces on the basis of milling with a rocking feed motion

In order to determine rational basic machining parameters of the milling process with a rocking feed motion, it is necessary to determine relationships between the coordinated motions.

The cutting edge turns by an angle φ_Z equal to 2π radians in one tool revolution around the *OZ* axis. During the same time τ, the tool turns around the *OY* axis by an angle φ_Y expressed in radians according to formula:

$$\varphi_Y = \frac{Z \times S_t \times p}{\frac{D}{2} - r}, \tag{1}$$

where *Z* is the number of the tool teeth; S_t is the feed per tool tooth, mm/tooth; *p* is the slip ratio; *D* is the tool diameter, mm; *r* is the radius of toroidal working surface, mm.

The tool feed is determined from formula:

$$S_0 = \frac{S_{Y_0} + S_{Z_0} + S_{KP}}{n_p}, \tag{2}$$

where S_0 is the technologically set feed per tool turn, mm/rev; S_{Y0} is the feed along the *OY* axis, mm/rev per tool revolution; S_{Z0} is the feed along the *OZ* axis, mm/rev per tool revolution; S_{KP} is the circular feed of the workpiece, mm/rev; n_p is the number of revolutions of the tool, min^{-1}.

$$S_{KP} = \pi \times D_w \times n_w, \tag{3}$$

where D_w is the workpiece diameter, mm; n_w is the number of the workpiece revolutions, min^{-1}.

The tool feeds along *SY* axis and across *SZ* axis of the machined profile (Fig. 8) for the concave arcuate surface area when the workpiece turns by angle ψ are determined from formulas:

$$\begin{cases} S_{Z_0} = p \times z \times (R_A + r_0) \times \cos\psi_i, \\ S_{Y_0} = p \times z \times (R_A + r_0) \times \sin\psi_i, \end{cases} \tag{4}$$

where R_A is the part radius at point *A* (Fig. 8); r_0 is the radius of the toroidal working surface of the tool; *p* is the slip factor.

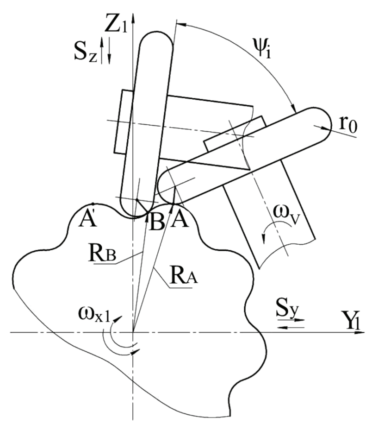

Fig. 8. Schematic of non-linear rolling of a geometrically complex cross section of the part

Respectively, velocities of the shaping motions being the first derivatives of displacement in time, $V = d_S/d_t$, are determined from formulas:

$$\begin{cases} \omega_{E1} = \dfrac{\psi}{t}, \\ V_{SZ} = p \times (R_A + r_0) \times \omega_{x1} \times \sin(\omega_{x1} \times t), \\ V_{SY} = p \times (R_A + r_0) \times \omega_{x1} \times \cos(\omega_{x1} \times t). \end{cases} \tag{5}$$

Establishment of functional interrelation between individual shaping motions reduced to establishment of displacements of a certain point of the cutting tool edge, ΔSZ, ΔSY, in increments depending on the angle of turn of the workpiece, ψi.

Moreover, these motions should take place in such a way that the tangent to some point of the tool profile coincide with the tangent to the machined side of the part cross section.

4. 1. Modeling the tool motion path

It is a rather difficult problem for some functions to determine the derivative. In this case, the angle of inclination close to the tangent at the point M_1 is determined from formula:

$$\alpha = \operatorname{arctg}\frac{Z_2 - Z}{Y_2 - Y}, \quad (6)$$

where Y_2, Z_2 are the coordinates of the next point after the M_1 point when moving around the part profile; Y, Z are coordinates of the previous point when moving around the part profile.

The function is checked for accuracy of the profile machining, that is, for accuracy of concurrence of the approximated tangent to the actual one at the M_1 point.

For this purpose, signs of the logical formula of the part are determined for two points located on the approximated tangent on both sides of the M_1 point at an equal distance Δt from it.

Value of Δt is determined by accuracy of the profile machining, $\Delta T \approx S/2$, where S is the size of the raster grid step.

Coordinates of the checking points on the tangent are determined from formulas:

$$\begin{cases} Z_{T1} = Z_1 + \Delta T\cos\alpha, \\ Y_{T1} = Y_1 + \Delta T\sin\alpha, \end{cases}$$

$$\begin{cases} Z_{T2} = Z_1 - \Delta T\cos\alpha, \\ Y_{T2} = Y_1 - \Delta T\sin\alpha. \end{cases} \quad (7)$$

Coordinates of the checking points are substituted in the logical formula of the part. In the event that both values have the same sign or are equal to zero, then this fully satisfies conditions of accuracy. For example, if both signs are positive, the machined surface has a convex shape in this section and concave if both signs are negative. At zero values of the logical formula, the profile has a rectilinear shape.

Next, points are selected one after the other from the multitude of the part's contour points starting from the first one and connected in a series with the points of the working surface of the tool from the multitude of MTs, starting from the priority ones. For example, the priority point n of the tool (Fig. 9) relates to a certain M_1 point on the profile of the machined surface having initial coordinates (Z_1, Y_1) and then the tool is adjusted by the angle $\Delta\varphi'$ conditioned by formula:

$$\Delta\varphi' = S \times p_n \times \frac{z+1}{R_i \times z}, \quad (8)$$

where S is the circular tool feed, mm/tooth; p_n is the slip factor; R_i is the radius of the tool's working point, mm, z is the number of machined grooves in the face section of the part.

When the tool turns clockwise by the angle $\Delta\varphi'''$ which is equal to:

$$\Delta\varphi''' = \Delta\varphi' + 180°. \quad (9)$$

When the tool turns counterclockwise, it must be turned by the following angles:

$$\Delta\varphi'' = 180° - \Delta\varphi',$$

$$\Delta\varphi''' = 180° + \Delta\varphi''. \quad (10)$$

Thus, the condition of the tool touching the surface to be machined is ensured.

To fulfill the condition of non-undercut, new coordinates of the M_0' and M_0'' points are determined when the tool touches the machined surface M_1 (Fig. 9).

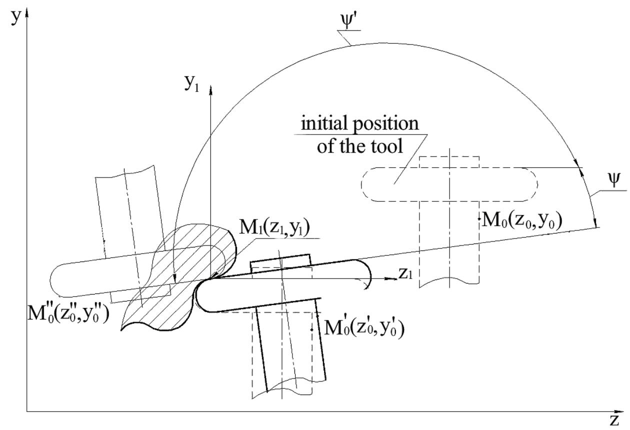

Fig. 9. Ensuring the condition of touching a point on the nominal surface with the tool's point chosen by priority

The working profile of the stamping mold (Fig. 10) described by arcs of circles of different radii was selected as an experimentally obtained surface.

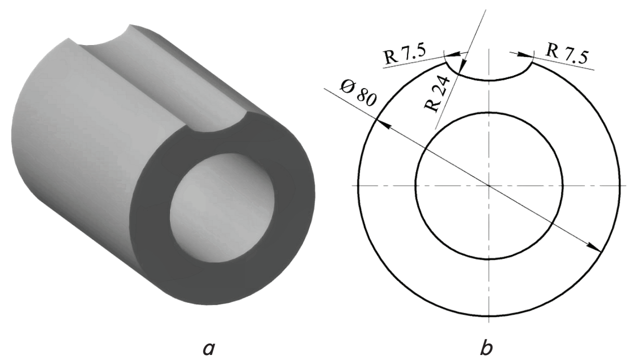

Fig. 10. Machined profile: model (*a*); dimensioned sketch (*b*)

To determine such chip parameters as volume, mass, cross-sectional area necessary for determining the specific productivity of machining, capabilities of R-functions should be used.

4. 2. Studying the parameters of cut-off layers using *R*-functions

Chips are formed by intersection of two adjacent positions of the mill and the workpiece (Fig. 11). A chip element is presented in Fig. 12.

It is seen from Fig. 13 that area of the cut-off metal layer is in the region bounded by three functions f_1, f_2, f_3.

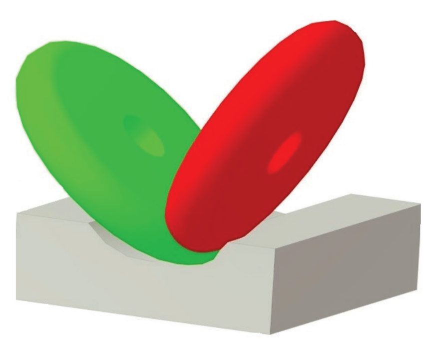

Fig. 11. Three-dimensional functional model of chip formation by a disk tool with a toroidal working surface

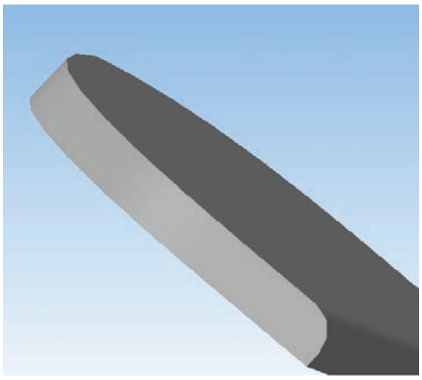

Fig. 12. Elementary volume of a chip

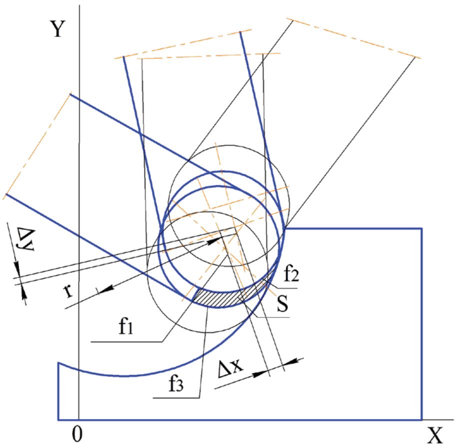

Fig. 13. Schematic of formation of a cut-off layer when milling with a reciprocatively rocking feed motion

Rvachev's algebrologic R-functions are used to develop a model of the process of chip formation during milling with a reciprocatively rocking feed motion and determine parameters of the cut-off layer. For this purpose, the elementary layer of metal cut off by each tooth is described by the logical formula obtained as a result of intersection of the three functions f_1, f_2, f_3 of positions of the two neighboring mill teeth and the machined surface (Fig. 13).

For the chip element shown in Fig. 14, the logical formula takes the form:

$$L = f_1 \wedge f_2 \wedge f_3,$$

$$\begin{cases} f_1 = x^2 + y^2 - R_\Pi^2, \\ f_2 = \left(x - \left(R_M - r\right)\right)^2 + y^2 - r^2, \\ f_3 = r^2 - \left(x - \left(R_M - r - \Delta x\right)\right)^2 - \left(y - \Delta y\right)^2, \end{cases} \qquad (11)$$

where R_M is the mill radius; r is the cutting insert radius; Δx, Δy are shifts along the x and y axes due to rotation, respectively.

Volume of the cut-off metal is determined using the method of experimental statistical simulation (Monte Carlo method) which consists in the following. An individual chip is formed when two traces of the tool modeled multiple times are superimposed. For this purpose, values of geometric parameters of the chip (h_{chip}, b_{chip} and f_{chip}) and values of geometric parameters of a certain cube to which the chip was reduced were raffled with the help of a random number generator according to the Norris distribution law.

The Monte Carlo method represents a way of volume determination by means of a pre-selected cube of known volume. Let us use cube $V = 2_r \times 2_r \times D_u/2$ (Fig. 15).

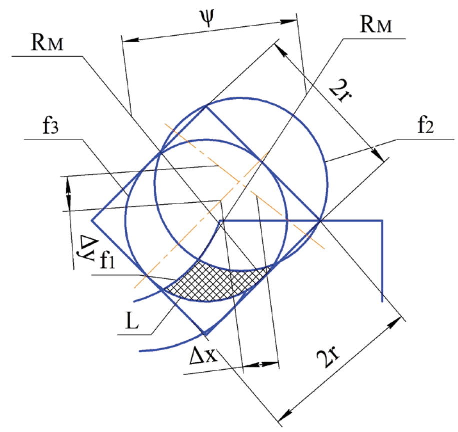

Fig. 14. Description of the element of the cut-off layer with the use of the algebra of logic

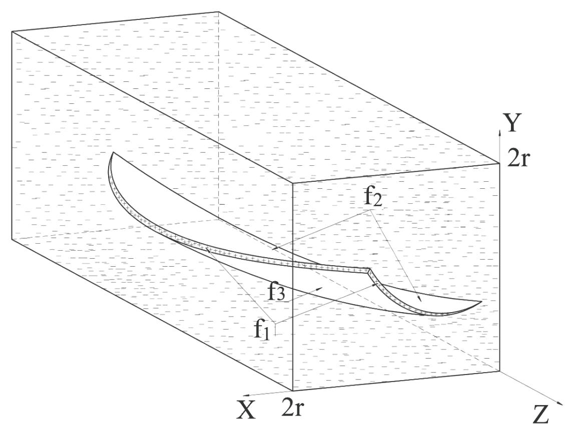

Fig. 15. Schematic of volume determination by the Monte Carlo method

When describing the chip by means of R-functions, value of 0 is decided at the boundary of the function domain. Values of the functions have positive sign inside the domain and negative outside the domain.

When substituting arbitrary values of arguments from the segment [0; 2r] for the three coordinates, the following values will be obtained: $L_{chip} > 0$; $L_{chip} < 0$ and $L_{chip} = 0$. Sum up the function values > 0 and divide their quantity by total number of the points used in calculation. Multiply the resulting number by the volume of initially specified cube to obtain volume of the cut-off material layer.

4. 3. Modeling the heat flows occurring in machining geometrically complex shaped surfaces by milling

Analysis of the thermophysical environment starts with consideration of heat exchange in the cutting zone when working with a simple cutting wedge since a tool of any shape and complexity consists of a system of simple cutting wedges.

A significant part of technological operations takes place under conditions of periodic cutting with periodization of the cutting process determined by its kinematics (in events of milling, slotting, planing, etc.) or intermittency of the machined surface (for example, when lathing spline shafts or rims of gear wheels). The intermittent cutting process makes it possible to reduce temperature of the tool contact surfaces. For example, during machining of CR18NI10TI grade steel with a hard alloy tool with inserts of TI15C6 grade steel in the region of conditions V=90÷270 m/min, t=0.5÷2 mm and S=0.07÷0.25 mm/rev, temperature of intermittent cutting with frequency f=1÷10 Hz is 20–30 % lower than in the event of continuous cutting.

The methods that combine regulation of length of the tool contact with the machined material are most effective at this time, that is, use of such machining methods in which breaks in the cutting process periodically occur.

Machining with multi-edge cutters (mills) with a reciprocatively rocking motion in the cutting plane is an effective way of controlling the heat emission capacity.

Such tool shift is realized by rotation of the working part of the disk mill with a radius profile relative to the center of the profile section of the toroidal surface. If the tool rotates around a certain point of the cutting edge with a frequency n_p, then any point located on the cutting edge will be in contact with the workpiece during time $\tau_p = \mu/(\varphi \times n_p)$ and will not come into contact with the workpiece during time $\tau_x = 1/n_p - \tau_p$. Because:

$$\mu = \frac{180}{\pi}\sqrt{\frac{t}{2\times r}},$$

where t is the cutting depth, mm; r is the radius of the working part of the tool, mm, then:

$$\tau_p = \frac{1}{\pi \times n_p}\sqrt{\frac{t}{2\times r}}.$$

Relation:

$$\frac{\tau_p}{\tau_p+\tau_x} = \frac{1}{\pi}\sqrt{\frac{t}{2\times r}}$$

characterizes the degree of non-stationarity of thermal process, and, consequently, the level of temperature of the cutting part of the tool. The less this ratio, the less important is the average temperature on the contact surfaces of the tool.

The reciprocatively rocking motion of the working part of the tool affects reduction of temperature in the cutting zone. Decrease in the heat emission is connected with the process non-stationarity as well as the fact that the sliding friction between the tool and the workpiece is partially replaced by the rolling friction.

Fixed shift of the cutting edge leads to reduction of work of deformation of the material in the cutting zone, and, consequently, to a decrease in the heat emission equivalent to this work. Distribution of the cutting heat between the workpiece, chips and a cutter changes significantly.

Assume the following conditions for an approximate calculation of the cutting temperature:

– the contact spot between the tool and the part has two surfaces;

– the scheme of the milling process is presented as interaction of two semi-bounded bodies contacting in a contact spot of *bxl* size (Fig. 16).

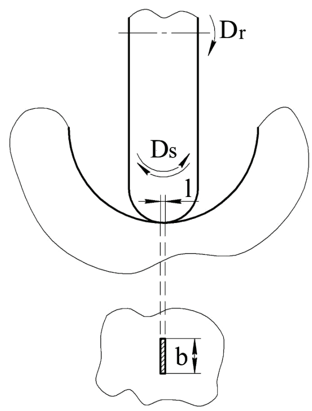

Fig. 16. Schematic of contact of the tool and the workpiece during milling with a reciprocatively rocking feed motion

Average cutting temperature is obtained by applying simple expressions for a source of limited width moving in a half-space with an adiabatic boundary region. A portion of intensity, q, of this source is transmitted in a quantity of $q_A = (l - b')\times q$ to the part and a portion in a quantity of $q_B = b'\times q$ is transmitted to the tool. For a permanently moving tool, average temperature of the contact surface calculated from the side of the part will be written as follows:

$$\bar{\theta} = \frac{4}{3}(1-b')\times q\frac{\sqrt{\omega\times l}}{\lambda\sqrt{\pi\times V}}K_c(u_1), \tag{12}$$

where V is the velocity of the main motion; ω, λ are the thermophysical characteristics of the machined material.

$$u_1 = \frac{b}{l}\sqrt{Pe} = \frac{b}{l}\sqrt{\frac{V\times l}{\omega}}. \tag{13}$$

For a tool that permanently performs reciprocatively rocking motion, average temperature of the contact surface is:

$$\bar{\theta} = \frac{4}{3}\times b'\times q\times\frac{\sqrt{\omega_p\times b}}{\lambda_p\sqrt{\pi\times V_2}}K_c(u_2). \tag{14}$$

Equate (12) and (14) to obtain the following:

$$b' = \frac{1}{1+\frac{\lambda}{\lambda_p}\times\sqrt{\frac{\omega_p}{\omega}}\times\sqrt{\frac{b}{l}}\times\sqrt{\frac{V}{V_2}}\times\frac{K_c(u_2)}{K_c(u_1)}}. \tag{15}$$

It can be seen from expression (15) that with an increase in circumferential velocity, V_2, of the tool, it receives an increasing portion of the heat generated during milling. By combining expressions (12) and (15) and given intensity of heat emission:

$$q = \frac{3.9\times P_z\times V}{b\times l}\ \text{cal/(cm}^2\text{s)},$$

a formula is obtained for approximate determining of the average temperature in the contact spot during reciprocal rocking motion of the tool:

$$\bar{\theta} = 0.72 \times \frac{P_z \times \sqrt{V \times \omega}}{\lambda \times b \times \sqrt{l}} \times$$
$$\times \frac{K_c(u_1)}{1 + \frac{\lambda_p}{\lambda} \times \sqrt{\frac{\omega_p}{\omega}} \times \sqrt{\frac{b}{l}} \times \sqrt{\frac{V}{V_2}} \times \frac{K_c(u_2)}{K_c(u_1)}}. \quad (16)$$

Force P_Z is determined from empirical dependence:

$$P_Z = 470 \times S_Z^{0.72} \times B \times z \times t_r^{0.86} / D^{0.86}. \quad (17)$$

As can be seen from formula (16), at low values of velocity V_2, temperature during reciprocal rocking motion is lower than during machining with a conventional tool. The increased heat dissipation in the body of the rocking tool (workpiece) is the main cause of temperature drop. This heat dissipation is described by coefficient b'.

For the purpose of checking the obtained regularities of average temperature on the contact surface, the milling process with a reciprocal rocking motion of feed was simulated. The computational methods used make it possible to calculate material deformations without distortion of the finite element grid.

Among various laws of material behavior at larger deformations, Johnson-Cook's elastic-thermo-viscoplastic law is the most common. It takes into consideration adiabatic shift phenomena caused by large plastic deformations and significant temperature gradients.

This law establishes dependence of stress σ on the degree of ε (%) and deformation rate as well as on temperature T and can be decomposed in a multiplicative form into three functions:

$$\sigma = (A + B \times \varepsilon^n) \times \left(1 + C \times \frac{\ln \varepsilon}{\varepsilon_0}\right) \times \left(1 - \left[\frac{T - T_0}{T_f - T_0}\right]^m\right), \quad (18)$$

where σ is the yield point; A is the limit of elasticity of the material under consideration; B and n are the linear and non-linear parameters of work hardening, respectively; ε is intensity of plastic deformations; C is the factor of sensitivity to the deformation rate; ε_0 is the linear expansion coefficient; T_f is the melting point; T_0 is the initial temperature.

The multipliers describe phenomenon of hardening, dynamic processes and phenomenon of temper, respectively.

Formation and separation of chips in the model is based on the law of material destruction which in its turn is based on the method of «erosion of elements» which consists in crack evolution and depends on the stress-strain state in the body of the worked part.

Application of this law includes two criteria. One of them characterizes the required degree of material destruction and the other is responsible for evolution of cracks, their propagation and separation of elements from each other.

The adapted criterion of destruction is interrelated with the Johnson-Cook law of motion. Destruction is considered for each element, beginning from the moment when:

$$\omega = \sum \frac{\Delta \bar{\varepsilon}}{\bar{\varepsilon}_f}, \quad (19)$$

where $\Delta\bar{\varepsilon}$ is the increment of the resulting plastic deformation, ε_f is the resulting deformation of material destruction.

The material destruction starts at $\omega = 1$.

The Johnson-Cook's model of destruction takes into consideration thermomechanical processes at high deformations. Critical magnitude of intensity of plastic deformation, ε_f^p is taken as a criterion of destruction. The equation of the resulting plastic deformation of destruction is as follows:

$$\varepsilon_f^p = \left[d_1 + d_2 \times \exp\left(d_3 \times \frac{J_1}{J_2}\right)\right] \times$$
$$\times \left[1 + d_4 \times \ln \frac{\bar{\varepsilon}^p}{\dot{\varepsilon}_0}\right] \times \left(1 + d_5 \times \frac{T - T_0}{T_f - T_0}\right), \quad (20)$$

where d_i is the material constant; J_1 is the mean stress; J_2 is the resultant Mises stress; $\bar{\varepsilon}^p$ is the design strain rate; $\dot{\varepsilon}_0$ is the limit characterizing the moment of sensitivity to the strain rate; T_f is the melting point; T_0 is the initial temperature.

In the event that the criterion of failure is fulfilled, the criterion of failure development comes into force. This criterion represents the level of energy, G_f, required for crack development. When the crack occurs, behavior of the material is represented by relation between stress and displacement but not between stress and strain.

The energy of destruction is determined by the formula:

$$G_f = \frac{K_C^2 - \left(1 - \upsilon^2\right)}{E}, \quad (21)$$

where K_c is the stability of destruction; E is the Young's modulus; ν is the Poisson factor.

The law of contact between the surface of the cutting tool and the machined surface is described by a combination of mechanical and thermal phenomena.

Mechanical phenomena are described by the model of friction:

$$|\sigma_t| \geq \mu - |\sigma_n|, \ \ |\sigma_t| < \mu - |\sigma_n|, \quad (22)$$

where σ_t, σ_n are the components of the contact stress vector, μ is the friction factor.

Thermal phenomena are represented by the coefficient of distribution of the heat flux generated by friction. In the simplified case, when two bodies are in a perfect contact, the Wernotta ratio can be described depending on the following relation between physical characteristics of the two materials:

$$\frac{\Phi_{g\to1}}{\Phi_{g\to2}} = \frac{\sqrt{\lambda_1 - p_1 - C_{p1}}}{\sqrt{\lambda_2 - p_2 - C_{p2}}}, \quad (23)$$

where λ_1 and λ_2 are the thermal conductivity, ρ_1 and ρ_2 are density, $C_{\rho1}$ and $C_{\rho2}$ are the specific heat conductivities of the cutting tool and the machined material, respectively.

Among the most commonly used software for modeling finite element cutting processes (Ansys, Advantedge, Deform 3D, Abaqus, etc.), Abaqus is of interest in the view of openness of the software code and the ability to integrate different laws of behavior of materials and their interactions.

An arbitrary Lagrange-Euler approach is used to simulate the cutting process by the finite element method.

Fig. 19 shows the results obtained in studies of temperature on the front surface of the tool.

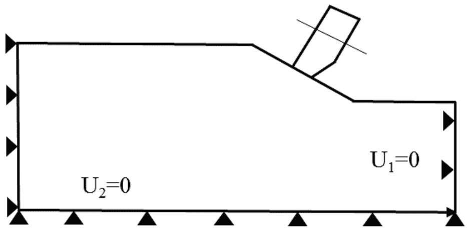

Fig. 17. Boundary conditions for a finite-element grid

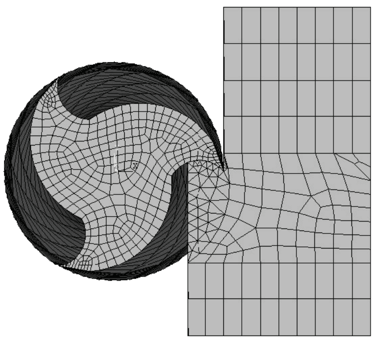

Fig. 18. A fragment of the calculation scheme and finite-element grids of the workpiece and the tool

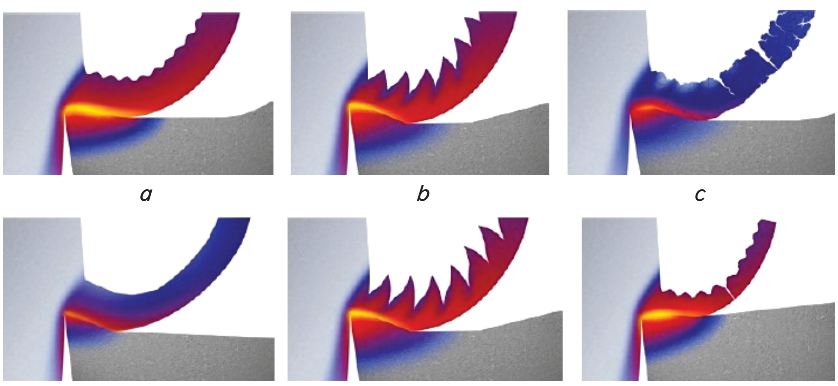

Fig. 19. Cutting temperature distribution in the tool at a change of the cutting speed, V, m/min; *Sz*=0.12 mm/tooth; V_{BL}=0.16 m/min; Steel 45: *V*=100 m/min (*a*); *V*=150 m/min) (*b*); *V*=200 m/min (*c*). Steel 9CRSI: *V*=100 m/min (*d*); *V*=150 m/min (*e*); *V*=200 m/min (*f*)

The finite element modeling gives a clear idea of temperature distribution during milling at a reciprocatively rocking motion of feed. In the future, this will allow us to investigate wear of the cutting edges of the tool for this type of milling.

5. Results obtained in the study of machining shaped surfaces of a complex profile by milling with a constant shift of the cutting edge

An analysis of the obtained results allows us to conclude that the cutting edge during milling with reciprocatively rocking motion of feed is heated more evenly and the length of the active part of the cutting edge creates heat removal favorable for the tool which has a beneficial effect on the wear resistance of cutting tools.

It was proved that the proposed method of machining mathematically complex shaped surfaces makes it possible to achieve reduction of temperature of the cutting tool edge by 27.5–31.5 % in comparison with conventional milling.

When analyzing the nature of tool wear during milling with reciprocatively rocking motion of feed, we can conclude that wear of the tool perimeter will be approximately the same. Wear of the back surface can be taken as a characteristic of wear resistance of the disk tool. At each turn of the tool, the cutting edge moves within the segment enclosed inside the angle of active contact, $\upsilon=\upsilon_1+\upsilon_2$. It is within this angle where the cutting edge wear occurs. Finally, parts of the angle of rotation of the working surfaces are in a contact with the cooling medium and, of course, do not wear out. In the reciprocatively rocking motion of feed, amount of wear accumulated by the cutting edge during time *T* will be determined from formula:

$$h_Z = L_p \times n_T \times S_Z \times h_{S.W.} \times T, \tag{24}$$

where h_T is the tool wear, mm; L_p is the length of the cutting path of a point on the cutting edge per one revolution of the mill, mm; N_r is the frequency of the reciprocatively rocking motion of feed, min^{-1}; S_z is the feed per tooth, mm/tooth; $h_{S.W.}$ is surface relative wear, μm/10^5 mm^2; *T* is time of the tool operation, min.

The cutting path L_P passed by the point of the cutting edge in a time corresponding to one revolution of the tool is determined.

In one revolution, the point of the cutting edge contacts with the cut-off layer during time τ and is determined from formula:

$$\tau = \frac{r \times \varphi^i_{\max}}{1000 \times V_{BK}}, \tag{25}$$

where *r* is radius of the tool profile, mm; $\varphi^i_{\max}$ is the maximum angle of contact of the tool with the workpiece; V_{BK} is velocity of relative reciprocatively rocking motion, m/min.

Time of one revolution is determined from formula:

$$\tau_0 = \frac{\pi \times r \times \varphi}{180000 \times V_{BK}}, \tag{26}$$

where *r* is the tool profile radius, mm; φ is the angle defining normal cutting conditions; V_{BK} is velocity of relative reciprocatively rocking motion, m/min.

Time of one revolution of the tool is determined from formula:

$$\tau_T = \frac{\pi \times D_T}{1000 \times V_P}, \tag{27}$$

where D_T is the tool diameter, mm; V_P is the cutting speed, m/min.

Velocity of the relative reciprocate rocking motion is expressed as follows:

$$V_{BK} = \frac{V_p \times r \times \varphi}{180 \times D_T}. \tag{28}$$

Thus,

$$\tau = \frac{9 \times \varphi^{i}_{\max} \times D_T}{50 \times V_p \times \varphi}. \tag{29}$$

The path passed by the point of the cutting edge per one tool revolution during time τ is determined by the formula:

$$L_p = \tau \times V_e = \frac{9 \times \varphi^{i}_{\max} \times D_T}{50 \times V_p \times \varphi} \times V_e, \tag{30}$$

where V_e is the actual cutting speed, m/min.

The proposed procedure of calculating the tool wear in processes of edge cutting machining with complex kinematics makes it possible to predict and determine wear of the cutting blades and determine on this basis the period of dimensional stability of the entire tool.

6. Discussion of results obtained in the study of the process of milling shaped surfaces on the basis of milling with a fixed shift of the cutting edge

The results obtained in the study show that the proposed method of machining geometrically complex shaped surfaces on the basis of milling with a fixed shift of the cutting edge, that is, with a reciprocatively rocking feed, makes it possible to increase the period of tool durability and productivity of milling due to the fixed kinematic shift of the cutting edge relative to the surface being machined. However, there are still some difficulties in using this machining method.

First, to implement this machining method, it is necessary to use 5-coordinate machining centers with a rotary table to transfer coordinated rotation of the workpiece which greatly complicates application of this method in practice.

Second, it should be understood that there are some features of compiling a control program for a CNC machine given that feed in this case has a reciprocatively rocking path.

It should also be noted that when choosing geometric elements to be machined, it is necessary to take into consideration position of the part and the workpiece relative to the zero point. The zero point is shifted relative to the model «binding» it to a separate geometric element of the geometric element.

7. Conclusions

1. The technical and technological solutions proposed in the study consist in development of a new highly effective method for machining geometrically complex shaped surfaces using disc radius mills with a reciprocatively rocking feed motion around the center of the profile section of the toroidal surface of the tool in the plane of motion in the machined profile. This makes it possible to increase the period of tool durability and milling performance due to the fixed kinematic shift of the cutting edge relative to the machined surface.

2. A mathematical apparatus for determining parameters of the cut off layers using algebra of logic (R-functions) and probabilistic statistical modeling (Monte-Carlo method) was developed. It establishes relationship between technological parameters of the process and productivity of milling with the reciprocatively rocking feed motion.

References

1. Petrushin S. I. Osnovy formoobrazovaniya rezaniem lezviynymi instrumentami: ucheb. pos. Tomsk: Izd. TGU, 2003. 172 p.
2. Reliability Analysis of Car Maintenance Scheduling and Performance / Tashtoush G. M., Tashtoush K. K., Al-Muhtaseb M. A., Mayyas A. T. // Jordan Journal of Mechanical and Industrial Engineering. 2010. Vol. 4, Issue 3. P. 388–393.
3. Radzevich S. P. Formoobrazovanie poverhnostey detaley. Rastan, 2001. 592 p.
4. Skorkin A., Kondratyuk O., Starchenko O. Theoretical bases of optimizing a tool idle motion while milling complex surfaces // Innovative Technologies and Scientific Solutions for Industries. 2018. Issue 4 (6). P. 62–70. doi: https://doi.org/10.30837/2522-9818.2018.6.062
5. Helleno A. L., Schützer K. Investigation of tool path interpolation on the manufacturing of die and molds with HSC technology // Journal of Materials Processing Technology. 2006. Vol. 179, Issue 1-3. P. 178–184. doi: https://doi.org/10.1016/j.jmatprotec.2006.03.092
6. Wei E.-J., Lin M.-C. Study on general analytical method for CNC machining the free-form surfaces // Journal of Materials Processing Technology. 2005. Vol. 168, Issue 3. P. 408–413. doi: https://doi.org/10.1016/j.jmatprotec.2004.11.009
7. Li J. G., Yao Y. X., Wang P. Assembly accuracy prediction based on CAD model // The International Journal of Advanced Manufacturing Technology. 2014. Vol. 78, Issue 5-8. P. 825–832. doi: https://doi.org/10.1007/s00170-014-6182-z
8. Zhang Z., Waszink A., Wijngaard J. An instrument for measuring TQM implementation for Chinese manufacturing companies // International Journal of Quality & Reliability Management. 2000. Vol. 17, Issue 7. P. 730–755. doi: https://doi.org/10.1108/02656710010315247
9. Yashchericyn P. I., Efremov V. D. Osnovy rezaniya materialov: ucheb. pos. Minsk: BGATU, 2008. 644 p.
10. Shalamov V. G., Smetanin S. D., Gatitulin M. N. Kinematika rotacionnogo i tradicionnogo rezaniya // Izvestiya Chelyabinskogo nauchnogo centra. 2009. Issue 3 (45). P. 13–17.
11. Wallner J., Pottman H. On the geometry of sculptured surface machining. Nashville, 2000. P. 417–432.
12. The Vehicle Routing Problem / P. Toth, D. Vigo (Eds.). Society for Industrial and Applied Mathematics, 2002. 367 p. doi: https://doi.org/10.1137/1.9780898718515
13. Pottmann H. General Offset Surfaces // Neural, Parallel & Scientific Computations. 1997. Vol. 5, Issue 1-2. P. 55–80.
14. Reznikov A. N., Reznikov L. A. Teplovye processy v tekhnologicheskih sistemah: ucheb. Moscow: Mashinostroenie, 1990. 288 p.
15. Tseng Y.-J., Joshi S. Determining feasible tool-approach directions for machining Bézier curves and surfaces // Computer-Aided Design. 1991. Vol. 23, Issue 5. P. 367–379. doi: https://doi.org/10.1016/0010-4485(91)90030-z